Proceedings Paper:

Nonde, L, Elgorashi, TEH and Elmirghani, JMH (2017) Virtual Network Embedding Employing Renewable Energy Sources. In: 2016 IEEE Global Communications Conference (GLOBECOM). 2016 IEEE Global Communications Conference (GLOBECOM), 04-08 Dec 2016, Washington DC USA. IEEE . ISBN 978-1-5090-1328-9

https://doi.org/10.1109/GLOCOM.2016.7842376

Virtual Network Embedding Employing Renewable Energy Sources

Leonard Nonde, Taisir E.H. Elgorashi and Jaafar M.H. Elmirgahni
School of Electronic and Electrical Engineering University of Leeds, LS2 9JT, United Kingdom

Abstract— Environmental sustainability in high capacity networks and cloud data centers has become one of the hottest research subjects. In this paper, we investigate the effective use of renewable energy and hence resource allocation in core networks with clouds as a means of reducing the carbon footprint. We develop a Green Virtual Network Embedding (GVNE) framework for minimizing the use of non-renewable energy through intelligent provisioning of bandwidth and cloud data center resources. The problem is modeled as a mixed integer linear program (MILP). The results show that it is better to instantiate virtual machines in cloud data centers that have access to abundant renewable energy even at the expense of traversing several links across the network. The GVNE model reduces the overall CO_2 emissions by up to 32% for the network considering solar power availability and data center locations.

Keywords—Cloud Networks; Renewable Energy, Virtual Network Embedding; Network Virtualization; MILP; Energy Efficient Networks; IP over WDM;

I. INTRODUCTION

Software Defined Networking (SDN) has brought about many possibilities in service provisioning in cloud networks. The fact that it is now possible to program a network on the fly as well as dictate how it behaves under different conditions provides opportunities for optimization of the physical resources that make up the network. A centralized control plane that is isolated from the data plane allows custom designed algorithms to dynamically route application specific flows or wavelengths in a network in order to fulfill a specific goal. As an example, an algorithm which automatically gives priority minimum hop routing for a live video stream at a particular time of the day and then tears it down when circumstances change can be implemented in the controller. In the absence of SDN, this process would have to be statically implemented and resources assigned even when they may not be used all the time.

In this work, the flexibility of centralized control of networks is used to reduce the carbon footprint of cloud infrastructure providers. An infrastructure provider (InP) in this case is the owner of a multi-tenant network that hosts various heterogeneous enterprise clients' virtual networks (VNs). A VN is composed of several virtual nodes and virtual links connecting these nodes. In the process of mapping VNs, the InP should satisfy both node (e.g. CPU and storage) and link (e.g. bandwidth and delay) demands of a virtual network request (VNR). The efficient provisioning of resources therefore presents a problem which is commonly known as the virtual network embedding (VNE) problem. Substantial work has been done on solving the NP-Hard VNE problem [1]. The VNE problem has been investigated with the objective of minimizing energy consumption by means of resource consolidation in [2], [3] and [4]. This is necessitated by the fact that there is a huge increase in the use of cloud computing services which are putting a huge stress on energy resources in both data centers and the high capacity IP/optical networks that connect them. In [5] we proposed an energy efficient virtual network embedding approach for cloud computing networks where power savings are introduced by consolidating resources in the network and data centers. We addressed the link embedding problem as a multilayer problem that includes both the IP layer and the optical layer in an IP over WDM network and considered the granular power consumption of various network devices as well as the power consumption in data centers. In [6], we extended our study to investigate the energy efficiency of VNE in optical OFDM networks and in [7] we studied the impact of maximizing profit on the power consumption and acceptance of VNRs.

The use of renewable energy in cloud networks is becoming an urgent requirement for InPs as the regulations surrounding the amount of CO_2 emissions are becoming stringent in this era of environmental sustainability. Very few studies have addressed the problem of reducing the greenhouse gas (GHG) emissions of InPs hosting VNs. The authors in [8] have developed an energy aware hybrid VNE approach where VNs are assigned to nodes with the cleanest energy sources. The authors have used CO_2 emission factors of cities as the determinant of where nodes are embedded. The city with the least factor becomes the most attractive. Whereas this approach seems reasonable in mitigating CO_2 emissions, it fails short of making full use of renewable energy that may be available in a city because it is possible that a city with a comparatively high CO_2 emission factor could also have a high availability of renewable energy. In this work we reduce the carbon footprint of cloud infrastructure by tapping into the available renewable energy sources to power the network and data centers. To address this goal, a green virtual network embedding (GVNE) approach that minimizes the use of non-renewable energy in core networks with clouds is proposed. We develop a mixed integer linear programming (MILP) model to minimize non-renewable power consumption. The MILP model determines how to effectively use renewable energy during the mapping of VNRs and whether to embed virtual nodes locally or to move them to distant data centers with abundant solar energy resources. The model results are a benchmark for heuristics and algorithms that would be developed and implemented in the control plane of an SDN based core network architecture with clouds.

The rest of this paper is organized as follows: The MILP model for green virtual network embedding in core networks with clouds is introduced in Section II. We analyze the key results and performance of the model in Section III. The paper is concluded in Section IV.

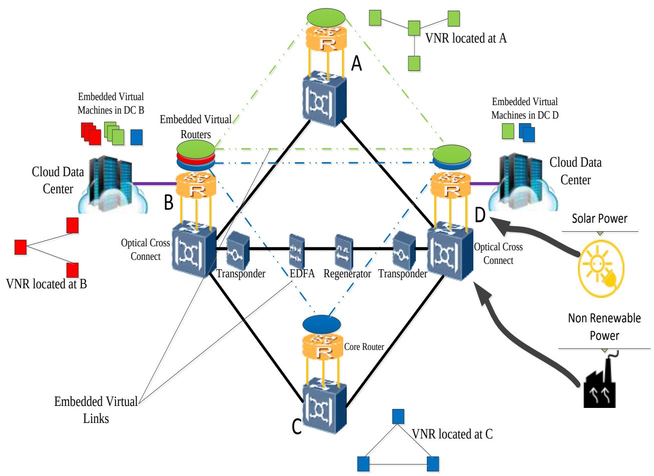

Fig.1: Virtual Network Embedding in an IP over WDM Network with Cloud Data Centers

II. MILP MODEL FOR GREEN VIRTUAL NETWORK EMBEDDING

The VNE problem defines how virtualized resources should be realized onto the substrate network. In Fig. 1, the VNRs green, red and blue with node and link demands are to be embedded onto the substrate IP over WDM network [5], [9] with data centers. The nodes of the substrate network have access to hybrid power supplies being composed of non-renewable energy and renewable energy. The renewable energy can be used to power the data centres and the IP over WDM equipment to reduce the total CO_2 emission of an IP over WDM network. The nodes with access to renewable energy also need access to non-renewable energy to guarantee QoS in the absence of renewable energy.

In this section we extend the energy efficient VNE MILP model we developed in [5] where our goal was to minimize the overall power consumption of VNE in IP/WDM core networks with data centres through resource consolidation. Here, the problem becomes that associated with minimizing the non-renewable energy consumption of VNE in the hybrid-power IP over WDM network. The model should be intelligent enough to decide whether to embed virtual resources in a locally based data center or to seek out a distant data center that has more renewable energy resources. This decision, takes into account the network power consumption that would be consumed if the virtual machines were embedded in a distant data center.

The substrate network is modeled as a weighted undirected graph $G = (N, L)$ where N is the set of substrate nodes and L is the set of substrate links. Each node or link in the substrate network is associated with its own resource attributes. The VNR v is represented by the graph $G^v = (R^v, L^v)$ where R^v is the set of virtual nodes made up of virtual machines and/or virtual routers and L^v is the set of virtual links.

In the following we reintroduce the sets, parameters, variables and constraints defined in [5] for completeness and introduce the new objective functions, parameters, variables and constraints developed to model the new GVNE approach.

Sets:

V	Set of VNRs
R	Set of nodes in a VNR
N	Set of nodes in the substrate network
N_m	Set of neighbor nodes of node m in the optical layer

Parameters:

s and d	Source and destination of a traffic demand in a VNR
b and e	End points of a link in the virtual network
i and j	End points of a virtual link in the IP layer
m and n	End points of a physical fiber link in the optical layer
LOC_b^v	$LOC_b^v = 1$ if the master node of VNR v must be located at substrate node b, otherwise $LOC_b^v = 0$
α	The virtual nodes consolidation factor which defines the maximum number of virtual nodes of a VNR that can be co-located at a substrate node.
β	The virtual machines consolidation factor which defines the maximum number of virtual machines of a VNR that can be co-located in a data center
μ	Power consumption per CPU core
NDC	The total number of data centers in the network
$C^{v,s}$	The number of virtual cores requested by virtual machine s of VNR v
DP_b	$DP_b = 1$ if substrate node b is a data center, otherwise $DP_b = 0$
$H^{v,s,d}$	Bandwidth requested by VNR v on virtual link (s,d)
B	Wavelength rate
W	Number of wavelengths per fiber
$D_{m,n}$	Length of the physical link (m,n)
$EA_{m,n}$	Number of EDFAs in physical link (m,n). Typically $EA_{m,n} = \left\lfloor \left(\frac{D_{m,n}}{S}\right) - 1 \right\rfloor + 2$, where S is the distance between two neighboring EDFAs
$EG_{m,n}$	The number of regenerators on a physical link (m,n). Typically $EG_{m,n} = \left\lfloor \left(\frac{D_{m,n}}{RG}\right) - 1 \right\rfloor$, where RG is the reach of the regenerator.
PR	Power consumption of a router Port
PT	Power consumption of a transponder
PE	Power consumption of an EDFA
RG	Power consumption of a regenerator
SE_m	Solar power capacity at node m

Variables:

$\delta_b^{v,s}$	$\delta_b^{v,s} = 1$, if node s of VNR v is embedded in substrate node b, otherwise $\delta_b^{v,s} = 0$.
Ψ^v	$\Psi^v = 1$, if all the nodes of a VNR v are fully embedded in the substrate network, otherwise $\Psi^v = 0$
$\rho_{b,e}^{v,s,d}$	$\rho_{b,e}^{v,s,d} = 1$, if the embedding of virtual nodes s and d of virtual request v in substrate nodes b and e, respectively is successful and a link b,e is established if a virtual link s,d of VNR v exists.
$\omega_{b,e}^{v,s,d}$	$\omega_{b,e}^{v,s,d}$ is the XOR of $\delta_b^{v,s}$ and $\delta_e^{v,d}$, i.e. $\omega_{b,e}^{v,s,d} = \delta_b^{v,s} \oplus \delta_e^{v,d}$
$L_{b,e}$	Total traffic demand on virtual link (b,e) due to the embedded links of all VNRs
Φ^v	$\Phi^v = 1$, if all the links of VNR v are fully embedded in the substrate network, otherwise $\Phi^v = 0$
$L_{i,j}^{b,e}$	Bandwidth demand of link (b,e) in the virtual network passing through the lightpath (i,j) in the substrate network
$C_{i,j}$	Number of wavelengths in lightpath (i,j) in the substrate network
$\varpi_{m,n}^{i,j}$	The number of wavelengths of lightpath (i,j) passing through a physical link (m,n)
$\lambda_{m,n}$	Number of wavelengths in physical link (m,n)
$\lambda_{m,n}^{(S)}$	Number of wavelengths in physical link (m,n) powered by renewable energy
$\lambda_{m,n}^{(NR)}$	Number of wavelengths in physical link (m,n) powered by non-renewable energy
$F_{m,n}$	Number of fibers in physical link (m,n)
$\Delta_b^{v,s}$	$\Delta_b^{v,s} = 1$ if virtual machine s of VNR v has been embedded at data center node b otherwise $\Delta_b^{v,s} = 0$
C_b	Total number of virtual cores embedded at data center b
$C_b^{(S)}$	Number of cores embedded at node b powered by renewable energy
$C_b^{(NR)}$	Number of cores embedded at node b powered by non-renewable energy

The network power consumption under non-bypass where lightpaths passing through an intermediate node are terminated and forwarded to the IP router as calculated in [10] is given as:

Power consumption of router ports:

$$\sum_{m\in N}\sum_{n\in N_m}\lambda_{m,n}\cdot PR$$

Power Consumption of transponders:

$$\sum_{m\in N}\sum_{n\in N_m}PT\cdot\lambda_{m,n}$$

Power Consumption of regenerators:

$$\sum_{m\in N}\sum_{n\in N_m}RG\cdot\lambda_{m,n}\cdot EG_{m,n}$$

Power Consumption of EDFAs:

$$\sum_{m\in N}\sum_{n\in N_m}PE\cdot EA_{m,n}\cdot F_{m,n}$$

We have only considered the power consumption in data centers due to the embedded virtual cores which is given as;

$$\sum_{b\in N}C_b\ \cdot\mu$$

The power consumption due to cooling, lighting and power supplies inside the data center has not been considered in this work. This assumption is adequate for the scope of this work because it has been shown in [11] that the workload variation in CPUs is the main contributor to the power consumption variations in a server and therefore the power consumption variations in the data center.

Objective:

Minimize total non-renewable power consumption given as:

$$\sum_{m\in N}\sum_{n\in N_m}\lambda_{m,n}^{(NR)}\cdot PR+\sum_{m\in N}\sum_{n\in N_m}\lambda_{m,n}^{(NR)}\cdot PT+\sum_{m\in N}\sum_{n\in N_m}EG\cdot\lambda_{m,n}\cdot RG_{m,n}+\sum_{m\in N}\sum_{n\in N_m}PE\cdot EA_{m,n}\cdot F_{m,n}+\sum_{b\in N}C_b^{(NR)}\cdot\mu$$

Subject to:

Node Embedding Constraints:

$$\sum_{v\in V}\sum_{s\in R}C^{v,s}\cdot\Delta_b^{v,s}\ \le C_b\qquad\forall b\in N\qquad(1)$$

Constraint (1) ensures that the virtual cores embedded in a data center do not exceed the capacity of the data center.

$$\sum_{b\in N}\delta_b^{v,s}\le 1\quad\forall v\in V,\ \forall s\in R\qquad(2)$$

Constraint (2) ensures that a virtual node is either rejected or only embedded once in a substrate network.

$$\sum_{b\in N}\Delta_b^{v,s}\le 1\qquad\forall v\in V,\qquad\forall s\in R\qquad(3)$$

Constraint (3) ensures that each virtual machine is either rejected or only embedded once in a data center.

$$DP_b\cdot\delta_b^{v,s}=\Delta_b^{v,s}\quad\forall v\in V,\forall b\in N,\forall s\in R\qquad(4)$$

Constraint (4) ensures that virtual machines are only embedded in nodes with data centers.

$$\sum_{s\in R}\delta_b^{v,s}\le\ \alpha\qquad\forall v\in V,b\in N\qquad(5)$$

Constraint (5) defines how many nodes belonging to the same request can be co-located on the same substrate node.

$$\sum_{s\in R}\Delta_b^{v,s}\le\ \beta\qquad\forall v\in V,b\in N\qquad(6)$$

Constraint (6) defines how many virtual machines belonging to the same request can be co-located in the same data center.

Link Embedding Constraints:

$$\delta_b^{v,s}+\delta_e^{v,d}=\omega_{e,b}^{v,d,s}+2\cdot\rho_{b,e}^{v,s,d}$$
$$\forall\ v\in V,\qquad\forall b,e\in N,\qquad\forall s,d\in R: s\neq d\qquad(7)$$

Constraint (7) ensures that virtual nodes connected in the VNR are also connected in the substrate network. We achieve this by introducing a binary variable $\omega_{e,b}^{v,d,s}$ which is only equal to 1 if $\delta_b^{v,s}$ and $\delta_e^{v,d}$ are exclusively equal to 1 otherwise it is zero.

$$\sum_{v\in V}\sum_{s\in N}\sum_{d\in N:s\neq d}\mathrm{H}^{v,s,d}\cdot\ \rho_{b,e}^{v,s,d}\ =\ L_{b,e}\ \forall b,e\in N\qquad(8)$$

Constraint (8) generates the traffic demand matrix resulting from embedding the VNRs in the substrate network and ensures that no connected nodes from the same VNR are embedded in the same substrate node.

$$\sum_{b\in N}\sum_{s\in R}C^{v,s}\cdot\delta_b^{v,s}=\Psi^v\sum_{s\in N}C^{v,s}\quad\forall v\in V\qquad(9)$$

Constraint (9) ensures that nodes of a VNR are completely embedded.

$$\delta_b^{v,1}=\ LOC_b^v\qquad\forall v\in V,b\in N\qquad(10)$$

Constraint (10) fixes the client's location in the network to the first node of the VNR.

$$\sum_{b\in N}\sum_{e\in N}\sum_{s\in R}\sum_{d\in R:s\neq d}\mathrm{H}^{v,s,d}\cdot\ \rho_{b,e}^{v,s,d}\ =\ \Phi^v\ \sum_{s\in R}\sum_{d\in R:s\neq d}\mathrm{H}^{v,s,d}$$
$$\forall v\in V\qquad(11)$$

Constraint (11) ensures the bandwidth demands of a VNR are completely embedded.

$$\Phi^v\ \ =\Psi^v\qquad\forall v\in V\qquad(12)$$

Constraint (12) ensures that both the nodes and links of a VNR are completely embedded. Constraints (9), (11) and (12) collectively ensure that a request is not partially embedded.

Flow conservation in the IP Layer:

$$\sum_{j\in N:i\neq j}L_{i,j}^{b,e}-\sum_{j\in N:i\neq j}L_{j,i}^{b,e}\ =\ \begin{cases}L_{b,e} & if\ \ i=b\\ -L_{b,e} & if\ \ i=e\\ 0 & otherwise\end{cases}$$
$$\forall b,e\in N: b\neq e\qquad(13)$$

Constraint (13) represents the flow conservation constraint for the traffic flows in the IP Layer.

Lightpath capacity constraint

$$\sum_{b\in N}\sum_{e\in N:b\neq e}L_{i,j}^{b,e}\ \le\ C_{i,j}\cdot B\qquad\forall i,j\in N: i\neq j\qquad(14)$$

Constraint (14) ensures that the sum of all traffic flows through a lightpath does not exceed its capacity.

Flow conservation in the optical layer

$$\sum_{n\in N_m}\varpi_{m,n}^{i,j}-\sum_{n\in N_m}\varpi_{n,m}^{i,j}=\begin{cases}C_{i,j} & if\ m=i\\ -C_{i,j} & if\ m=j\\ 0 & otherwise\end{cases}$$
$$\forall i,j\in N: i\neq j\qquad(15)$$

Constraint (15) ensures the conservation of flows in the optical layer.

City ID / Time	1	2	3	4	5	6	7	8	9	10	11	12	13	14
	SR: 05:14	SR: 05:43	SR: 05:16	SR: 05:54	SR: 05:27	SR: 05:55	SR: 05:51	SR: 05:39	SR: 05:17	SR: 05:53	SR: 05:18	SR: 05:41	SR: 06:27	SR: 05:30
	SS: 21:02	SS: 20:04	SS: 19:34	SS: 20:40	SS: 20:41	SS: 20:10	SS: 20:53	SS: 20:47	SS: 20:24	SS: 19:56	SS: 20:30	SS: 20:29	SS: 20:30	SS: 20:59
	Seattle	Palo Alto	San Diego	Salt Lake	Boulder	Houston	Lincoln	Champaign	Pittsburg	Atlanta	Ann Arbor	Ithaca	College Pk	Princeton
00:00	0.0kW	0.0kW	0.0kW	0.0kW	0.0kW	0.0kW	0.0kW	0.0kW	0.0kW	0.0kW	0.0kW	0.0kW	0.0kW	0.0kW
02:00	0.0kW	0.0kW	0.0kW	0.0kW	0.0kW	0.0kW	0.0kW	0.0kW	0.0kW	0.0kW	0.0kW	0.0kW	0.0kW	0.0kW
04:00	0.0kW	0.0kW	0.0kW	0.0kW	0.0kW	0.0kW	0.0kW	0.0kW	0.0kW	0.0kW	0.0kW	0.0kW	0.0kW	0.0kW
06:00	0.0kW	0.0kW	0.0kW	0.0kW	0.0kW	0.0kW	0.0kW	0.0kW	0.0kW	0.0kW	1.5kW	14.3kW	0.0kW	75.3kW
08:00	0.0kW	0.0kW	0.0kW	0.0kW	27.0kW	10.9kW	8.2kW	5.1kW	125.3kW	1.4kW	4.6kW	171.5kW	54.8kW	903.6kW
10:00	0.3kW	412.6kW	412.6kW	8.1kW	81.1kW	130.3kW	98.4kW	12.3kW	271.4kW	4.1kW	9.9kW	371.6kW	158.3kW	1957.8kW
12:00	2.3kW	2063.2kW	2063.2kW	15.1kW	175.7kW	282.4kW	213.1kW	36.9kW	375.8kW	12.2kW	15.2kW	571.6kW	243.5kW	3012.0kW
14:00	4.1kW	3713.8kW	3713.8kW	20.9kW	270.2kW	434.4kW	327.8kW	36.9kW	375.8kW	12.2kW	9.9kW	371.6kW	158.3kW	1957.8kW
16:00	4.1kW	3713.8kW	3713.8kW	20.9kW	243.2kW	391.0kW	295.1kW	26.7kW	271.4kW	8.8kW	5.7kW	214.4kW	91.3kW	1129.5kW
18:00	2.9kW	2682.2kW	2682.2kW	20.9kW	175.7kW	282.4kW	213.1kW	16.4kW	167.0kW	5.4kW	3.8kW	142.9kW	60.9kW	753.0kW
20:00	1.8kW	1650.6kW	1650.6kW	9.3kW	108.1kW	173.8kW	131.1kW	6.2kW	62.6kW	1.4kW	1.5kW	57.2kW	24.4kW	301.2kW
22:00	0.6kW	619.0kW	103.2kW	4.6kW	27.0kW	10.9kW	49.2kW	0.0kW	0.0kW	0.0kW	0.0kW	0.0kW	0.0kW	0.0kW

Table I: Solar Power Availability in Different Cities. SR: Sunrise, SS: Sunset, recorded in individual cities in June [15]

Physical Link capacity constraints

$$\sum_{i\in N}\sum_{j\in N:i\neq j} \varpi_{m,n}^{i,j} \leq W \cdot F_{m,n}$$
$$\forall m \in N, n \in N_m \quad (16)$$

$$\sum_{i\in N}\sum_{j\in N:i\neq j} \varpi_{m,n}^{i,j} = \lambda_{m,n}$$
$$\forall m \in N, n \in N_m \quad (17)$$

Constraints (16) and (17) represent the physical link capacity constraints. Constraint (16) ensures that the number of wavelengths in a physical link does not exceed the capacity of fibers in the physical links. Constraint (17) gives the total number of wavelength channels used in a physical link.

$$C_b = C_b^{(S)} + C_b^{(NR)} \quad \forall b \in N \quad (18)$$

Constraint (18) calculates the total number of cores in a data centre as the sum of the embedded cores powered by renewable energy and the embedded cores powered by non-renewable energy.

$$\lambda_{m,n} = \lambda_{m,n}^{(S)} + \lambda_{m,n}^{(NR)} \quad \forall m, n \in N \quad (19)$$

Constraint (19) calculates the total number of wavelength in fiber link as the sum of the wavelengths powered by renewable energy and the wavelengths powered by non-renewable energy.

$$\sum_{n\in N_m} \lambda_{m,n}^{(S)} \cdot PR + \sum_{n\in N_m} \lambda_{m,n}^{(S)} \cdot PT + C_m^{(S)} \leq SE_m \ \forall m \in N \quad (20)$$

Constraint (20) ensures that the total renewable energy consumption by router ports, transponders and data centers at each node does not exceed the maximum renewable power available for the node. Due to the location of EDFAs and regenerators in between nodes, it has been assumed that they only have access to non-renewable energy.

III. PERFORMANCE EVALUATION

The performance of the GVNE MILP model is examined using the NSFNET reference network topology. The network has 14 nodes and 21 links as shown in Fig. 2. VNRs come from enterprise clients from all the nodes in the network. The enterprise client's location is fixed but the requested virtual nodes could be embedded in any data center in the cloud. The concentration of clients at any substrate node is based on the population of the states where the node is located (see Fig. 2). In the case of California where we have two cities in one state (nodes 2 and 3), we have evenly distributed the population of the state between the two cities.

The VNRs consist of virtual processing demands in terms of number of virtual CPU cores and bandwidth demands of virtual links connecting the virtual nodes. A total of 50 enterprise clients send VNRs to the InP over a 24 hour period at two hour time granularity of service. The traffic generated by the VNRs over a 24 hour period is modelled according to the 2020 average business Internet traffic between nodes in the NSFNET network as projected by the GreenTouch Consortium [12]. The requests once accepted stay in the network for 2 hours after which they will be torn down and adjusted according to the new arriving demands. The number of virtual nodes per VNR is uniformly distributed between 1 and 5 and the number of virtual cores per VNR is uniformly distributed between 1000 and 8000. The substrate network is un-capacitated in terms of both node and link resources. The consolidation factors are set to $\alpha = \beta = 5$, i.e. all the virtual nodes and machines of a VNR can be co-located. The current and future criterion for designing cloud infrastructure is to distribute the content among a number of data centers to minimize the delay experienced by the users and to avoid the scenario of having a single hot node in the network. The NSFNET contains five data centers located at nodes (2, 3, 6, 8 and 10) [12].

We consider solar energy as the source of renewable energy. The solar power availability profile for nodes is shown in Table I. The solar power data is obtained from the Open PV Project [13] of the National Renewable Energy Laboratory of the United States of America. It provides detailed data of the total installed photovoltaic capacity of each individual state in the United States. The data from the Open PV Project shows the total installed solar capacity for each state which has contributions from residential areas, private industries and utilities. The data obtained from the U.S. Energy Information Administration [14] shows that approximately 20% of the solar installed capacity is from utilities. We have assumed that the cloud InP has access to 1% of this solar power as well as non-renewable power (Fig. 1) through the utility in each node. Since the output power of solar energy sources varies at different times of the day, we use the sunrise and sunset data used by the authors in [15] to work out the available solar power at any given two hour intervals as a fraction of the maximum installed capacity. Table II shows the values of the parameters that have been used in the model.

The AMPL software with the CPLEX 12.5 solver is used as the platform for solving the MILP models on a PC with an Intel® Xeon™ CPU, running at 3.5 GHz, with 64 GB of RAM. The running times for the model averages 15 minutes for each time point. Fig. 3 shows the overall non-renewable power consumption and solar power consumption of the GVNE model at different times of the day. It can be observed that despite having an increase in the CPU cores and bandwidth demand between 06:00 hours and 12:00

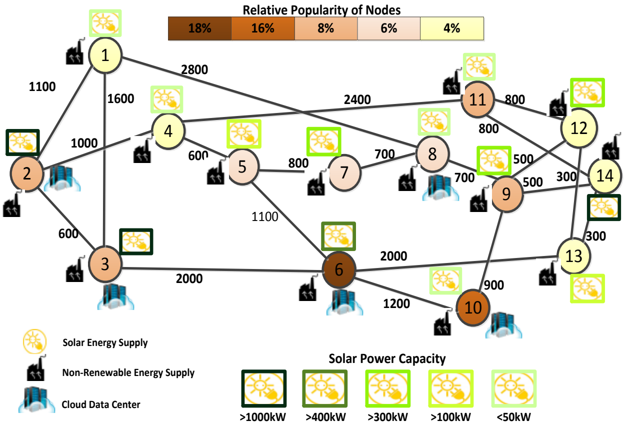

Fig. 2: NSFNET Network with popularity and solar capacity information

Table II: Parameters used in the model

Distance between two neighboring EDFAs (S) [16]	80 (km)
Distance between two neighboring Regenerators (RG)[17]	2000 (km)
Number of wavelengths in a fiber (W) [18]	32
Wavelength Rate (B)	40Gbps
Power consumption of a transponder (PT) [16]	167 (W)
Power consumption of a regenerator (RG) [19]	334 (W)
Power consumption of a 40Gb/s router port (PR) [17]	850(W)
Power consumption of an EDFA (PE) [16]	55 (W)
Power consumption per CPU core [20]	11.25(W)

hours, the non-renewable power consumption continues to decrease as expected due to the increasing availability of solar power. In order to adequately serve the further increase in load from the VNRs, there is a subtle increase in non-renewable power consumption from 14:00 hours until 20:00 hours and thereafter, there is a sharp increase in non-renewable power consumption due to the dwindling solar energy supply during this period. The non-renewable power consumption curve without access to solar energy follows the traffic profile throughout the day. The overall reduction in CO_2 emissions in this scenario achieved by GVNE is 32%.

In the interest of clearly understanding what is happening in the network, in Fig. 4 we examine the individual non-renewable and solar power consumption contributions for both data centers and the network. Fig. 4(a) shows that the power consumption in data centers has the most significant influence on how the embedding of VNRs is done in all the data centers. The model maximizes the savings in the amount of consumed non-renewable power by consolidating the embeddings in data centers with abundant solar power even at the expense of using more non-renewable power in the network as can be seen in Fig. 4(b). Whereas the non-renewable power consumption in data centers drastically falls between 06:00 hours and 14:00 hours, the non-renewable power consumption in the network shows a steady increase. The average reduction in CO_2 emissions in data centers and the network is 35% and 15% respectively compared to the scenario with no access to renewable energy. This picture is made much clearer by looking at how the embedded CPU cores for various VNRs are distributed across the five data centers in the network.

Fig. 5(a) shows the embedding of virtual cores in the different data centers under the scenario with no access to renewable energy. The most popular destination for

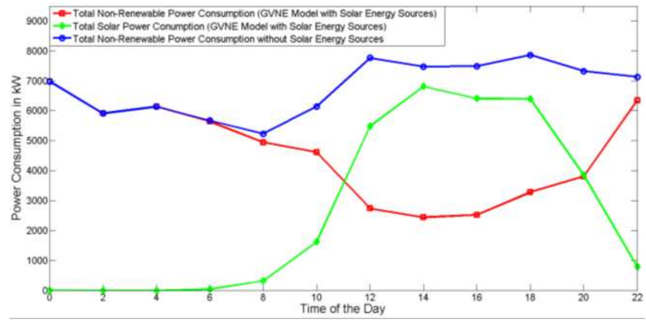

Fig. 3: Total Solar and Non-Renewable Power Consumption

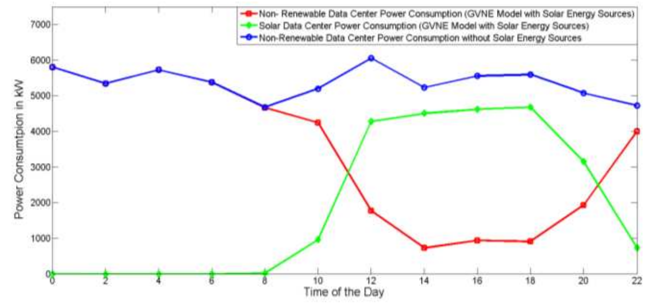

Fig. 4(a)

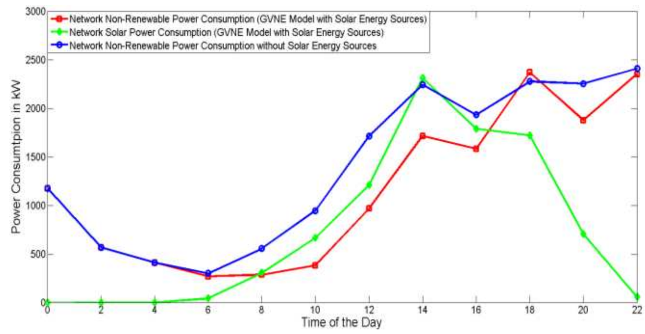

Fig. 4(b)

Fig. 4: Non-Renewable and Solar Power Consumption in (a) Data Centers, (b) Networking Components

embedded virtual machine workloads is in the data center at node 6 (Houston) due to its relatively high nodal degree and the high concentration of VNRs located at the node itself and those connected to it. The data center in node 3 (San Diego) does not get a high utilization at any time of the day. The data centers in nodes 2 (Palo Alto) and 3 (San Diego), do not surpass the data center in node 6 in utilization at any time during of the day. This picture however changes when solar energy is introduced in the network. Fig. 5(b) shows that the GVNE model embeds a high proportion of virtual machines in nodes 2 and 3 which hosted only a minimal amount when solar energy sources are not considered. A large proportion of virtual cores which would normally be embedded in data centers located at nodes 6, 8 and 10 at periods between 12:00 hours and 20:00 hours are taken up by the data centers in nodes 2 and 3 which have abundant solar energy at these periods. Figs. 5(c) and 5(d) show the distribution of embedded cores in the five data centers powered by non-renewable energy and solar energy, respectively. The little or no use of solar energy at data centers in nodes 8 and 10 (Fig. 5(d) is due to the fact that these nodes have very minimal solar energy. It is therefore optimally used for routing traffic demands to data centers in nodes 2 and 3 where more savings can be accrued by tapping into the abundant renewable energy sources.

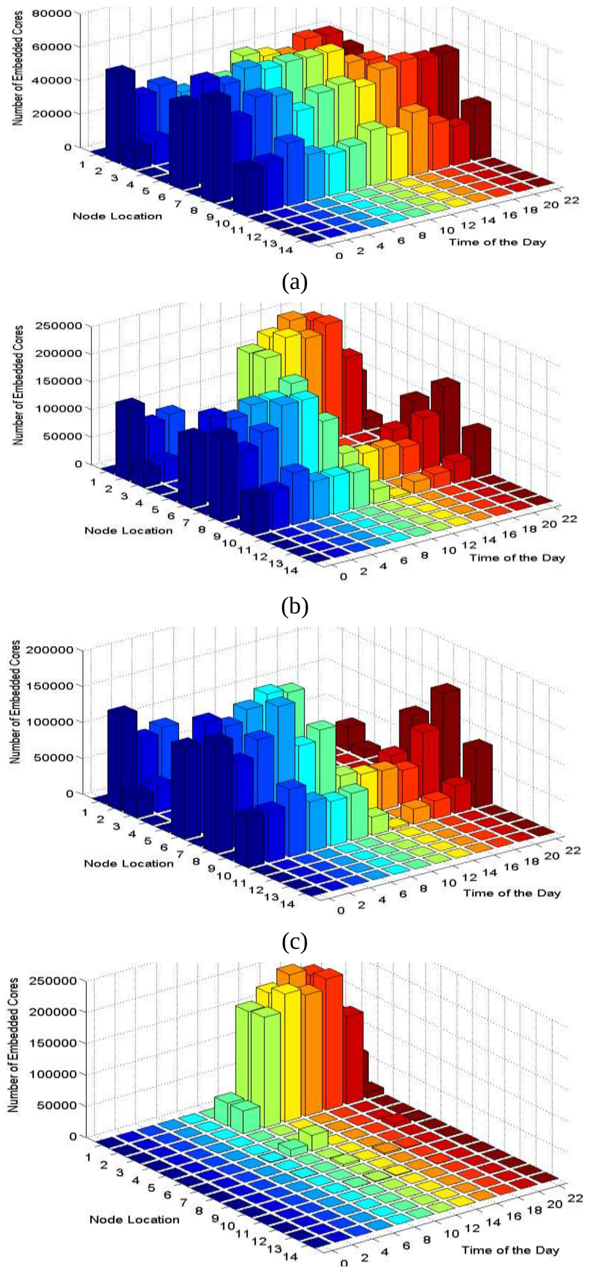

Fig. 6: Embedded Cores Distribution in Data Centers, (a) Supplied only by non-renewable energy sources (Reference case), (b) GVNE supplied by both non-renewable and solar energy sources, (c) Non-renewable energy powered cores under GVNE (d) Solar energy powered cores under GVNE

IV. CONCLUSIONS AND FUTURE WORK

This paper has investigated the effective use of renewable energy sources to reduce the CO_2 emissions of the cloud service provisioning of infrastructure as a service. The results of the GVNE MILP model developed show that it is better to instantiate virtual machines in cloud data centers that have access to abundant renewable energy even at the expense of traversing several links across the network. An overall reduction in CO_2 emissions of 32% is achieved for the scenario that has been chosen. Completely focusing on reduction of non-renewable power consumption has the potential to significantly increase the overall OPEX associated with electricity consumption considering the geographical price discrimination of electricity. It is therefore necessary to develop a framework that addresses both concerns of reducing electricity costs and GHG emissions. In the case of delay sensitive applications, such as live video streaming, embedding a virtual node running such an application in a distant data centre that has abundant renewable energy, would cause serious quality of service problems. It is therefore expected that each enterprise client would send a request to the InP with specific delay requirements. Our future work will investigate and address all these concerns. We will also develop real time heuristic algorithms and implement them on an SDN based experimental test bed.

V. REFERENCES

[1] D.G. Anderson, "Theoretical Approaches to Node Assignement," 2002 [cited 13/10/2015]; Available from: http://repository.cmu.edu/cgi/viewcontent.cgi?article=1079&context=compsci

[2] B. Wang; X. Chang; J. Liu, J.K. Muppala, "Reducing power consumption in embedding virtual infrastructures," IEEE Globecom Workshops (GC Wkshps), 2012, pp.714, 718, 3-7 Dec. 2012

[3] J.F. Botero, et al., "Energy Efficient Virtual Network Embedding," IEEE Communication Letters, 2012. **16**(5): p. 756-759.

[4] S. Sen, et al., "Energy-aware virtual network embedding through consolidation," in IEEE Computer Communications Workshops (INFOCOM WKSHPS). 2012.

[5] L. Nonde, T.E.H. El-Gorashi, and J.M.H. Elmirghani, "Energy Efficient Virtual Network Embedding for Cloud Networks", IEEE Journal of Lightwave Technology, 2015. **33**(9): p. 1828-1849

[6] L. Nonde, T.E.H. El-Gorashi, and J.M.H. Elmirghani, "Green Virtual Network Embedding in Optical OFDM Cloud Networks," in 16th IEEE Conference on Transparent Optical Networks (ICTON), 2014.

[7] L. Nonde, T.E.H. El-Gorashi, and J.M.H. Elmirghani, "Cloud Virtual Network Embedding: Profit, Power and Acceptance," in proc. IEEE Global Comminications Conference (GLOBECOM), 2015.

[8] Triki, N., et al., "A green energy-aware hybrid virtual network embedding approach", Computer Networks, 2015. **91**: p. 712-737

[9] X. Dong, T.E.H. El-Gorashi, and J.M.H. Elmirghani, "Green IP Over WDM Networks With Data Centers", IEEE Journal of Lightwave Technology, 2011. **29**(12): p. 1861-1880.

[10] G. Shen and R.S. Tucker, "Energy-Minimised Design for IP Over WDM Networks" IEEE/OSA Journal of Optical Communications and Networking, , 2009. **1**(1): p. 176-186.

[11] X. Fan, W.D. Weber, and L.A. Barroso, "Power provisioning for a warehouse-sized computer," ACM SIGARCH Computer Architecture News, 2007. **35**(2): p. 13-23.

[12] J.M.H. Elmirghani, T. Klein, K. Hinton, T.E.H. El-Gorashi, A. Q. Lawey, X. Dong, **"**GreenTouch GreenMeter Core Network Power Consumption Models and Results," IEEE OnlineGreenComm 2014.

[13] NREL, "Open PV Sate Rankings." 2015; Available from: https://openpv.nrel.gov/rankings.

[14] EIA. 2015 [cited 2015 20/10/2015]; Available from: http://www.eia.gov/renewable/

[15] X. Dong., T.E.H. El-Gorashi, and J.M.H. Elmirghani, "IP Over WDM Networks Employing Renewable Energy Sources", IEEE Journal of Lightwave Technology, 2011. **29**(1): p. 3-14.

[16] Van Heddeghem, W., et al., "Power consumption modeling in optical multilayer networks," Photonic Network Communications, 2012. **24**(2): p. 86-102

[17] GreenTouch. "White Paper on GreenTouch Final Results from Green Meter Research Study." 2015; Available from: https://s3-us-west-2.amazonaws.com/belllabs-microsite-greentouch/uploads/documents/White%20Paper%20on%20Green%20Meter%20Final%20Results%20August%202015%20Revision%20-%20vFINAL.pdf

[18] Ciena. "DWDM vs. CWDM." Cited 2015; Available from: http://www.ciena.com/technology/dwdm-vs-cwdm/. 10 Oct 2015.

[19] Van Heddeghem, W., et al., "A power consumption sensitivity analysis of circuit-switched versus packet-switched backbone networks," Computer Networks, 2015. **78**(0): p. 42-56.

[20] Intel®. "Intel® Xeon® Processor E3-1200 v3 Product Family". Available from: http://www.intel.co.uk/content/dam/www/public/us/en/documents/product-briefs/xeon-e3-1200v3-brief.pdf